SAE TECHNICAL PAPER SERIES

2008-01-1132

Seam Welding and Cooling-Control Heat-Treatment of Martensitic Stainless Steel

Daniel S. Codd
KVA Incorporated

Reprinted From: Welding and Joining and Fastening, 2008 (SP-2196)

ISBN 978-0-7680-1634-5

9 780768 016345

**2008 World Congress
Detroit, Michigan
April 14-17, 2008**

SAE International™

400 Commonwealth Drive, Warrendale, PA 15096-0001 U.S.A. Tel: (724) 776-4841 Fax: (724) 776-0790 Web: www.sae.org

ISSN 0148-7191

Printed in USA

2008-01-1132

Seam Welding and Cooling-Control Heat-Treatment of Martensitic Stainless Steel

Daniel S. Codd
KVA Incorporated

ABSTRACT

From a production standpoint, many high-strength welded (GTAW, GMAW, laser, etc.) assemblies require post-weld mechanical forming operations. Complications often arise when using Advanced High Strength Steels (AHSS), whose chemical composition may lend it to fully martensitic, extremely brittle as-welded microstructures. Martensitic Stainless Steels (MSS) are a particular class of AHSS susceptible to high fusion and heat-affected zone (HAZ) hardness after welding.

The focus of this study is to provide a relatively straightforward way to improve the ductility of as-welded air-hardenable martensitic stainless steel joints without subjecting the weld to a separate costly and time-consuming off-line pre-or-post weld heat treatment. The additional ductility afforded by such a method can greatly expand the design opportunities using commercially available martensitic stainless alloys, which are capable of strengths in excess of 1400 MPa after a final solution heat treatment.

INTRODUCTION

Martensitic stainless steels (MSS), alloys primarily of chromium and carbon, possess a distorted body-centered cubic (bcc) or body-centered tetragonal (bct) martensitic crystal structure in the hardened condition. These alloys are ferromagnetic, hardenable by heat treatments and mildly corrosion resistant.

Historical applications of MSS include cutlery, surgical instruments, scissors, springs, valves, shafts, ball bearings, turbine equipment and petrochemical equipment.

The compositions of MSS, typically between 10.5 to 18 wt% chromium, are specifically formulated to render them amenable to a quench-and-temper (Q+T) heat treatment in order to produce high levels of strength and hardness. Although the chromium level is the same as in ferritic stainless steels (e.g. type 409), the higher carbon content of the martensitic grades results in a complete transformation from ferrite to austenite (γ) at high temperature, followed by a subsequent change to the hard martensite phase upon rapid cooling. MSS are considered "air-hardenable," as all but the thickest sections fully harden during an air-quench heat treatment cycle to room temperature.

The thermal cycle of heating and rapid cooling, which occurs within the fusion and HAZ during welding, is equivalent to a rapid air-cooling quench cycle. As a result, the martensitic weld structure that is produced is extremely brittle in the untempered condition. Regardless of the prior condition of the steel, annealed, hardened, or hardened and tempered, welding produces a hardened martensitic fusion zone and HAZ. (FIG. 1) Because of their response to welding thermal cycles, MSS are considered the most difficult of the five stainless steel families to weld.[1]

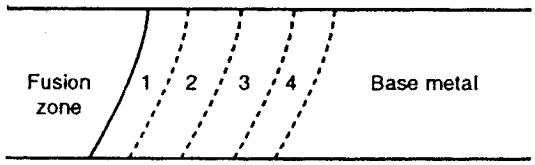

Four HAZ regions:

1 γ + ferrite ⟶ martensite + ferrite
2 Coarse-grained γ ⟶ martensite
3 Fine-grained γ ⟶ martensite
4 Overtempered base metal

FIG. 1 Four HAZ regions observed in martensitic stainless steel. γ represents austenite. *(from Ref. 1)*

However, MSS are ideally suited for structural components and assemblies, satisfying the requirements of high strength, toughness and corrosion resistance, with ease of forming in the annealed state.

Although most assemblies, once fabricated from these alloys, would undergo a final homogenizing solution heat-treatment hardening cycle, great benefits could be realized if the as-welded brittleness could be reduced. Secondary processes on weldments, such as cold working, bending, flanging or hydroforming (as in the

case of seam-welded tubing) could be performed with greater confidence and ease.

One method to reduce weld hardness is to add filler material, whereby the final metallurgy is modified in such a way that the percentage of hard and brittle components such as martensite is reduced.[2] Another approach is to heat-treat the welded part during or after welding. From a production point of view, heat treatment during production is preferred in order to avoid costly pre- or post-treatment.[3]

Typical off-line methods of controlling weld and HAZ hardness include secondary post-weld heat treatments (PWHT) such as process annealing. Pre-heating methods can be used to slow the rate of cooling, thereby reducing percentage of the martensitic phase present. Unfortunately, these methods are neither cost-nor-time effective for high production levels associated with modern manufacturing methods. Induction heat treatment has been known for many years to be an efficient way of heat-treating steel parts.[4] The simple in-line induction weld cooling-control and PWHT method presented here is shown to appreciably increase weld and HAZ ductility without increasing process time.

EXPERIMENTAL PROCEDURE

MATERIAL CHEMISTRY

Type 410 stainless steel (UNS41000 / SAE 51410) was selected for this investigation. Chemical composition for this alloy is shown in Table I. For all trials, the MSS sheets were welded in the annealed condition. Samples were run with 0.5, 1 and 2mm sheet thickness, with corresponding chemical analysis listed in Table II.

TABLE I. Type 410 stainless steel (UNS S41000) alloying elements nominal wt % (maximum values)

C	Mn	S	P	Si	Cr
0.15	1.00	0.03	0.04	1.00	11.5-13.5

TABLE II. Type 410 stainless steel chemical analysis wt % used in study

t (mm)	C	Mn	S	P	Si	Cr	Ni	Al	Mo	N
0.5	0.14	0.41	0.003	0.024	0.30	11.75	0.12	0.002	0.02	0.01
1	0.14	0.37	0.003	0.032	0.40	12.25	0.24	0.001	0.03	0.01
2	0.12	0.45	0.003	0.025	0.34	12.55	0.50	0.001	0.04	0.01

WELDING & COOLING-CONTROL APPARATUS

A linear-seam welding test fixture (FIG. 2) was designed to butt GTAW weld the test strips in 150cm lengths, from which test coupons were taken from the central, steady-state portion of the weld.

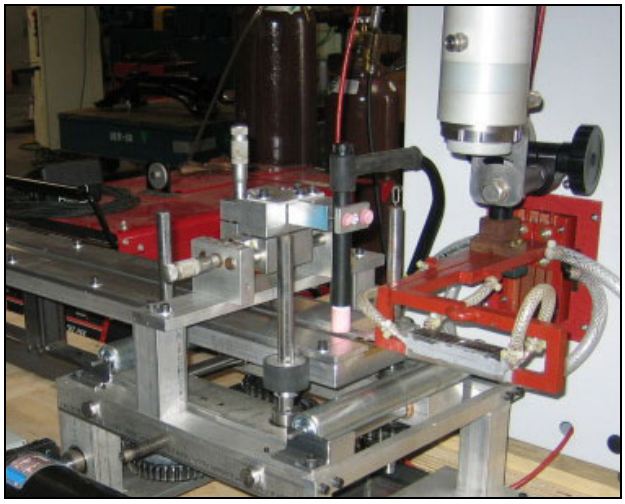

FIG. 2 Seam Weld/Cooling-Control test apparatus.

A specialized one-sided linear induction coil was implemented downstream of the GTAW torch body to control the cooling profile of the weld seam. The coil was designed with a ferrite concentrator to focus the high frequency energy into a linear pattern directed onto the weld seam. A split coil design with a novel through-coil sight bore allowed for direct surface temperature measurements using a non-contact 3.9µm wavelength infrared pyrometer. Figure 3 shows the dimensions of the induction coil.

The test strips, 5cm x 150cm, were supported with a clamping shuttle fixture, which also provided for a channel with a plurality of holes for root-side gas shielding. A Miller Maxstar 300 DX GTAW power supply was used with a water-cooled TIG machine torch with a gas lens collet. Tri-mix multidopant blend tungsten electrodes were used with 100% argon for the torch and root shield gas.

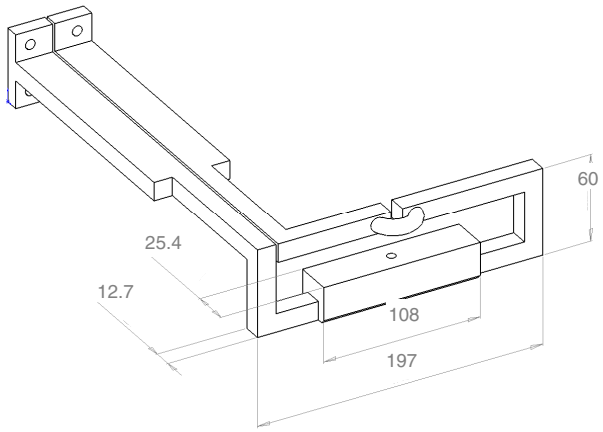

FIG. 3 Induction coil. Material travel is from left-to-right. (dimensions in mm)

Weld variables such as travel speed, tungsten tip geometry, welding current and arc voltage were experimented with to determine the optimal high-speed GTAW parameters, summarized in Table III. Experimentation was carried out using pulsed weld waveforms at various pulse frequencies (100 – 300 Hz) and duty cycles; however for the study a non-pulsed waveform was used. These baseline GTAW settings were maintained throughout the controlled-cooling trials to isolate the effects of the secondary heat source on the weld quality.

TABLE III. GTAW Welding parameters

t (mm)	Electrode dia. (in)	Electrode tip angle	Welding speed (mm/s)	Welding current (A)	Arc voltage (V)	Nominal heat input (J/mm)
0.5	1/16	15°	25.4	80	10	32
1	1/16	18°	19.1	150	13	100
2	3/32	20°	12.7	270	18	380

A water-cooled L.C. Miller Dyna-Flux 25kW induction power supply was used to energize the coil. Various parameters were experimented with, including induction power level, induction frequency, distance from induction coil to workpiece and downstream distance of the induction coil to the welding torch. A Raytek Marathon MMMT-series non-contact single color infrared pyrometer was mounted to take direct surface temperature readings of the weld seam beneath the induction coil. The temperature measuring location was situated at the midpoint of the induction coil's length.

EVALUATION

After welding, the test strips were quality assessed by means of visual inspection, qualitative bend testing and quantitative tensile testing. Longitudinal face bend testing was conducted according to ASTM E190: Standard Test Method for Guided Bend Test for Ductility of Welds. Specimens were sheared to size (20mm x 55mm, weld centered and parallel to length), bent and visually assessed for cracks. Test fixtures with bend radii of 2t and 4t were utilized.

Tensile test specimens were prepared and tested according to DIN EN 895: Destructive testing of welds in metallic materials. Specimens were sheared to rough size and then profiled on a CNC mill with a carbide cutter. The modified specimen dimensions, identical for both transverse and longitudinal tensile testing, are shown in FIG. 4. A Tinius Olsen 60K hydraulic universal testing machine was used to load the specimens to failure. A 25mm gage-length axial extensometer was used to measure strain as the load was applied, with strain and load data downloaded to a PC for analysis. A total of 230 samples were tested.

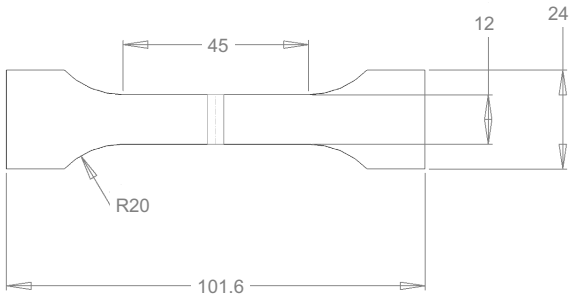

FIG. 4 Tensile specimen dimensions. (mm)

Selected samples were also subjected to a hardening (Q+T) cycle in a Cress C1232 Electric Box furnace prior to tensile testing. Specimens were heated to 1010°C, soaked for approximately 100 seconds, removed from the furnace and allowed to air quench. After the samples reached room temperature, a low-temperature tempering was performed at 175°C for 30 minutes, to simulate an electro-coating bake cycle.

PROCESS EVALUATION ON SEAM-WELDED TUBING

The induction heating apparatus was then moved to a continuous roll-forming tube mill, set up to produce GTAW seam-welded tubing using type 410 stainless strip. Two sizes of tubing were produced: ∅28.6mm OD x 0.5mm wall and ∅19.1mm OD x 1.2mm wall. Tubing was subjected to destructive mechanical testing to assess overall integrity and formability. ASTM A513 ring flaring tests, with a 60° included angle cone, were used in addition to ASTM E8 full-tube tensile testing. Figure 5 shows typical full-tube tensile specimen gripping methods that were used with 50mm gage lengths. Tubes were tested as-welded, with inductor cooling-control, and after a Q+T hardening cycle, for a total of 48 samples.

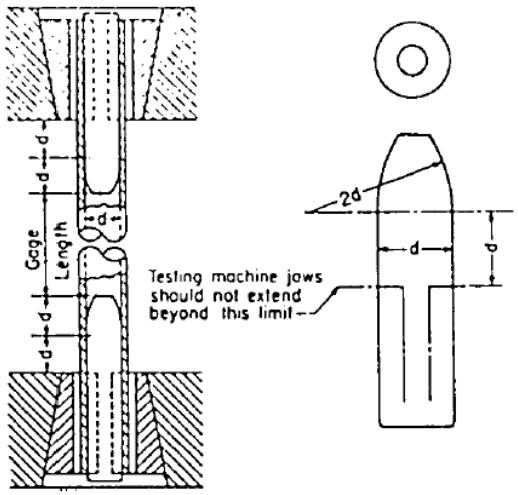

FIG. 5 Typical Full-tube tensile specimen grip fixture, *ASTM E8, section 6.9.1.*

RESULTS AND DISCUSSION

GUIDED BEND WELD DUCTILITY DATA

Figure 6 shows typical longitudinal face bend test samples after testing. Baseline control trials were run with no post-weld cooling control, and baseline process-annealed samples were run with a full-cooling to room temperature after welding followed by a seam annealing re-heat pass. Samples were tested to failure (weld seam cracking) or until a complete U-bend was formed. Figures 7 and 8 show representative load-displacement data for the tests.

As expected, more specimens survived the bend test in the 4t configuration than the more-severe 2t setup. All baseline as-welded trials exhibited cracking prematurely. Conversely, all baseline process-annealed samples completed the U-bend without cracking.

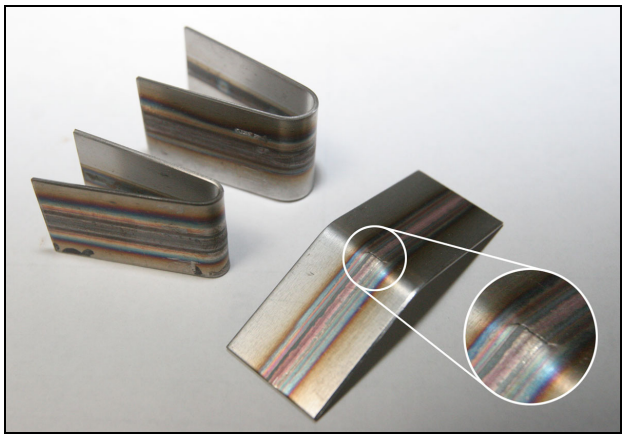

FIG. 6. Typical ASTM E190 guided bend-test weld ductility specimens. From left: 2t bend radius-full bend; 4t bend radius-full bend; 4t bend radius-failure

In varying the controlled-cooling trial parameters, it was found that two variables had greatest effect on the bend-test performance: downstream distance of the inductor coil and the induction power level. Ductility was improved with moving the inductor downstream and increasing the power level to heat the seam sufficiently. Optimal ductility improvements were found with the inductor centerline approximately 30.5cm downstream of the weld torch, and power level settings corresponding to average under-inductor seam temperatures around 650°C.

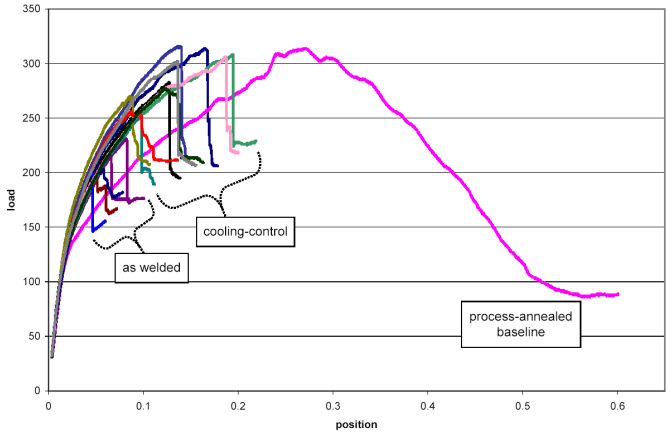

FIG. 7. Comparison of 3-point longitudinal face-bend test load-position data for various process conditions. Modified ASTM E190 guided bend test for ductility of welds. Bend Radius = 2t; t = 1mm.

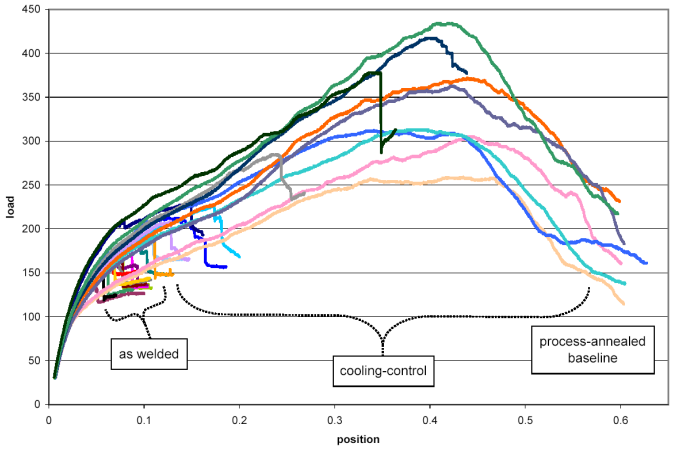

FIG. 8. Comparison of 3-point longitudinal face-bend test load-position data for various process conditions. Modified ASTM E190 guided bend test for ductility of welds. Bend Radius = 4t; t = 1mm.

OPTIMAL COOLING-CONTROL PARAMETERS

Table IV summarizes key induction heating parameters found for optimal weld ductility improvement. For all thicknesses, the average cooling-control (c.c.) seam temperature underneath the induction coil was found to be around 650°C, below the upper critical (A_{C3}) for type 410 stainless steel, which is approximately 960°C[5]. Tests performed at higher induction power settings, and consequently mean seam temperatures above A_{C3}, the upper critical fully-austenitized threshold, exhibited a decrease in ductility in the weld seam area. Conversely, tests performed at lower induction power settings, and lower mean seam temperatures, showed only slight increases in weld zone ductility.

TABLE IV. Optimal Induction Heat-treatment parameters

t (mm)	Inductor power	Coil Voltage (V)	Coil amperage (A)	Induction Frequency (kHz)	Net heat input to coil (kJ/mm)	Average seam temp (°C)
0.5	10%	57	156	96	0.35	635
1	18%	98	214	94	1.10	650
2	30%	111	223	94	1.95	730

These findings agree with well-known behavior of hardenable alloys: if the metal is heated above the lower critical temperature (A_{C1}), the temperature at which austenite starts to form, the newly formed austenite will harden upon subsequent cooling into martensite. Equation (1), originally developed for 13 wt% Cr steels with less than 0.05 wt% C, can be used to roughly predict the A_{C1} temperature in higher carbon alloys:[5]

$$A_{C1}(°C) = 850 - 1500(C+N) - 50Ni - 25Mn + 25Si + 25Mo + 20(Cr - 10) \quad (1)$$

For type 410 stainless composition used in this trial, the predicted A_{C1} temperature is approximately 675°C. This agrees well with the experimental results, i.e. maximum softening with inductor temperatures near the A_{C1} threshold, with increasing hardness at higher inductor mean temperatures due to the re-hardening of the weld seam.

TENSILE TEST DATA

Figure 9 shows sample elongation data versus under-inductor mean weld seam temperatures for two downstream locations of the induction coil for all three test strip thicknesses.

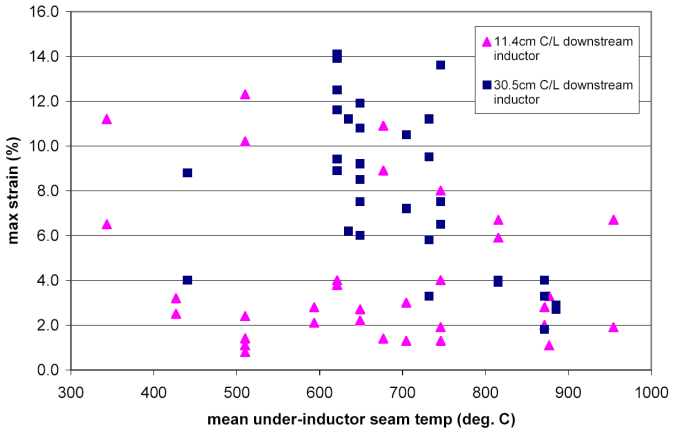

FIG. 9. Maximum Elongation vs. Mean Under-Inductor Weld Seam Temperature for varying downstream inductor coil distances: longitudinal weld seam specimens, all gauges.

Although the data from the induction coil immediately downstream of the welding torch (inductor centerline 11.4cm downstream of weld torch) is quite scattered, the samples with the induction coil further downstream (inductor centerline 30.5cm downstream of weld torch) show a significant improvement in maximum weld-seam strain at failure. Greatest ductility benefits were observed through induction heat-treatment near the A_{C1} temperature, 675°C.

The initial trial configuration, intended to slow the cooling rate of the weld seam in the 800-500°C range, with the inductor immediately downstream of the weld torch (11.4cm inductor location), did not produce significant softening of the HAZ at any power levels. Previous studies on other hardenable materials have verified the speed at which the temperature drops through this temperature range determines the final metallographic microstructure, and thereby the ductility of the material.[3] Some samples from this configuration actually showed a decrease in ductility when compared to the baseline welds. Much of the scatter in the 11.4cm data set can be attributed to the 0.5mm thickness tests, as the limited joint restraint on the 0.5mm strips may account for the negligible effect of the cooling-control at any power level for that case. Figure 10 shows sample elongation vs. temperature data for the 1mm and 2mm thicknesses only.

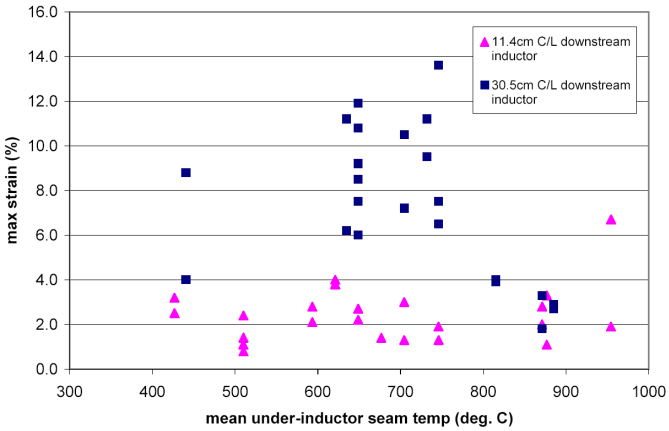

FIG. 10. Maximum Elongation vs. Mean Under-Inductor Weld Seam Temperature for varying downstream inductor coil distances: longitudinal weld seam specimens, **1mm & 2mm only**.

As shown in FIG. 11, the necessary hold time for producing a mixed A + F + C (austenite/ferrite/chromium carbide) microstructure in type 410 MSS is on the order of 200 seconds. The induction coil in the 11.4cm location, even operating at the correct temperatures to 'catch' the nose of the TTT curve, only holds the cooling weld seam near the proper temperature for approximately 10 seconds. Consequentially, with the inductor adjacent to the weld torch, the HAZ is never held at an intermediate temperature for sufficient time to promote the formation of the A+F+C microstructure directly from the molten weld pool.

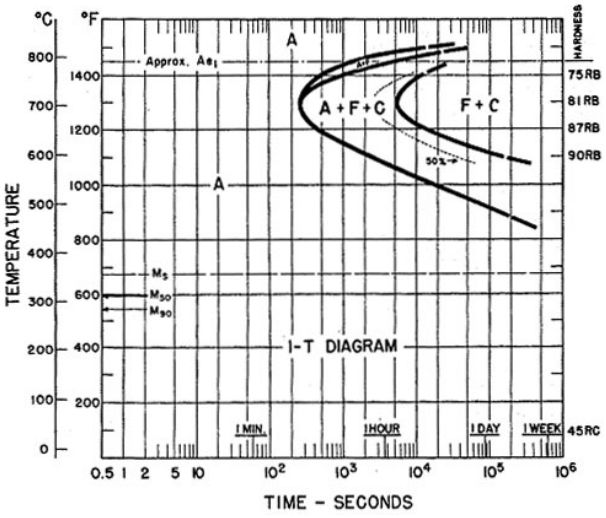

FIG. 11 Time-Temperature Transformation (TTT) Diagram for type 410 stainless steel *(from Ref. 6)*

Alternatively, with the inductor moved downstream from the weld torch, the weld pool is allowed the chance to cool below the martensite start (M_s) temperature, approximately 330°C for type 410 stainless steel.[5] The austenite in the weld seam is allowed to transform, at least partially, into martensite before being re-heated by the inductor. This inductor cooling-control, equivalent to an air-quench tempering cycle, promotes transformation of the martensite into ferrite and very fine carbides. This transformation reduces strength but improves ductility and toughness.[5] Additionally, the prolonged time at elevated temperatures increases diffusivity of hydrogen atoms while relieving thermal stresses, thereby reducing the probability of hydrogen-induced cracking or cold cracking. [5] Several downstream induction coil positions were experimented with before settling on the coil located approximately 30.5cm downstream of the weld torch, which was used for the entirety of the study.

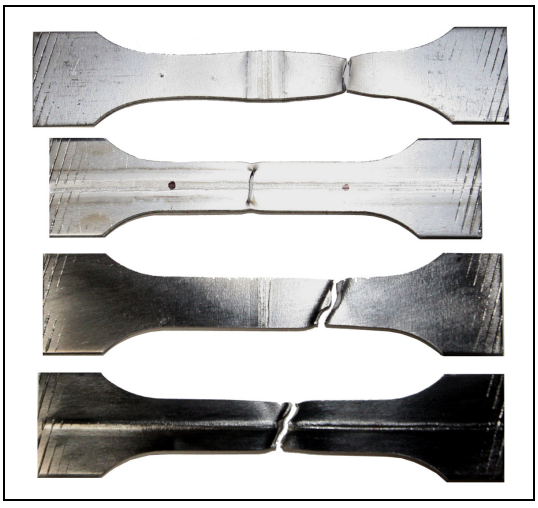

FIG. 12. Typical tensile-test weld specimen fracture locations. From top: Transverse (T), annealed base metal; Longitudinal (L), annealed base metal; T, post-weld C.C. & Q+T; L, post-weld C.C. & Q+T.

Figure 12 shows typical tensile test specimen fracture-locations. All transverse samples failed outside of the fusion and heat-affected zones for both the as-welded/cooling-control and the Q+T specimens. The as-welded/cooling control samples showed significant necking in the fracture zone, as expected with the annealed base metal properties. The as-welded/cooling-control longitudinal specimens typically exhibited brittle fracture in the fusion and HAZ regions that caused the surrounding base metal to yield, but not fail until further loading. The Q+T hardened longitudinal specimens failed simultaneously across the fusion/HAZ/base metal interfaces, propagating along angles of maximum principal stress.

Figures 13 and 14 show average results for longitudinal tensile testing of the baseline, optimal cooling-control, and Q+T weld specimens.

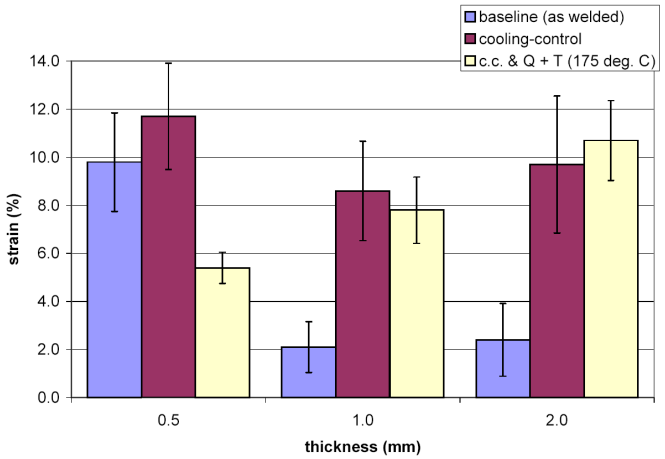

FIG. 13. Comparison of Maximum Strain at fracture for optimum process conditions. DIN EN 895 longitudinal tensile specimen, average results for 62 trials.

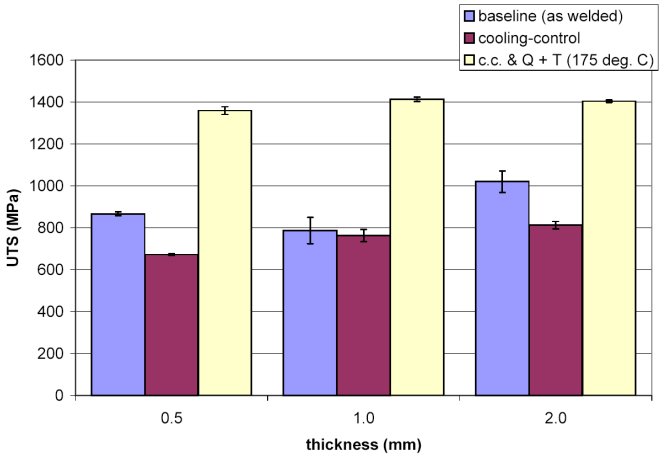

FIG. 14. Comparison of Ultimate Tensile Strength for optimum process conditions. DIN EN 895 longitudinal tensile specimen, average results for 62 trials.

For all thicknesses, the optimum induction coil's cooling-control methods on the weld seam resulted in an increase in maximum strain at fracture and a corresponding decrease in ultimate tensile strength when compared to the as-welded trials. The thicker gauges exhibit a better response to the controlled-cooling process; possibly due to the larger thermal inertia and therefore slower effective cooling-rate after the inductor. The cooling-control weld specimens that were subjected to a Q+T thermal cycle exhibited strengths near 1400 MPa, as expected for hardened type 410 stainless steel.

APPLICATION TO SEAM-WELDED TUBING

After the conclusion of the weld-strip testing, the cooling-control apparatus was installed on a seam-welded tube mill. (FIG. 15) The inductor was placed approximately 30cm downstream of the GTAW torch body and power settings were adjusted to bring the under-inductor seam temperature to 550°C - 650°C.

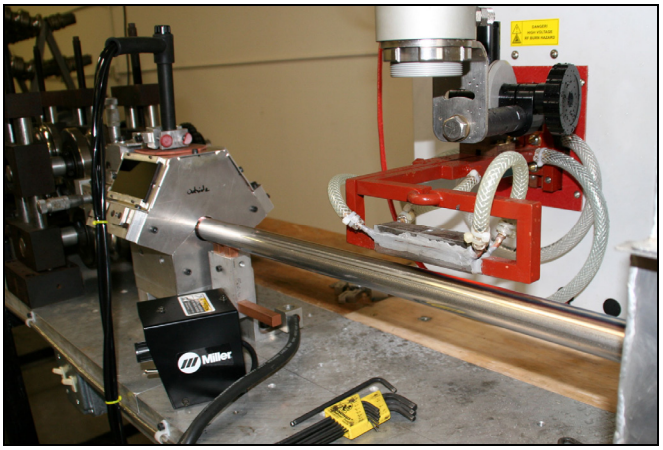

FIG. 15 Tube mill weld-zone with inductor installed, material travel from left-to-right.

Typical microhardness traverse data is shown in Figure 16. It is interesting to note that the width of the HAZ in the as-welded sample is well over 3mm. While not softened completely to the level of the base metal, the cooling-control significantly reduces the HAZ microhardness relative to the as-welded sample. Furthermore, after a Q+T heat treatment, the microhardness of the tube remains constant across the circumference, without any HAZ weakened areas.

Mechanical properties at fracture are shown in FIGS. 17 and 18. Similar to the butt-weld test strips, specimens run with inductor cooling-control showed an increase in total axial elongation, with a corresponding slight decrease in ultimate tensile strength. The Q+T solution heat-treated samples showed much less overall necking in the tube section, along with a markedly different angled fracture surface along the plane of maximum principal stress. Representative full-tube tensile specimens are shown in Figure 19.

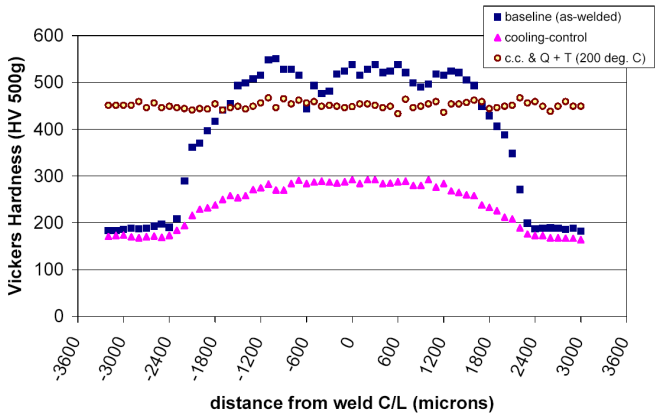

FIG. 16. Typical Vickers Microhardness Profile: Load: 500 g; Hardness Spacing: 100 µm; Seam-Welded ∅19.1 x 1.2mm UNS41000 Tubing.

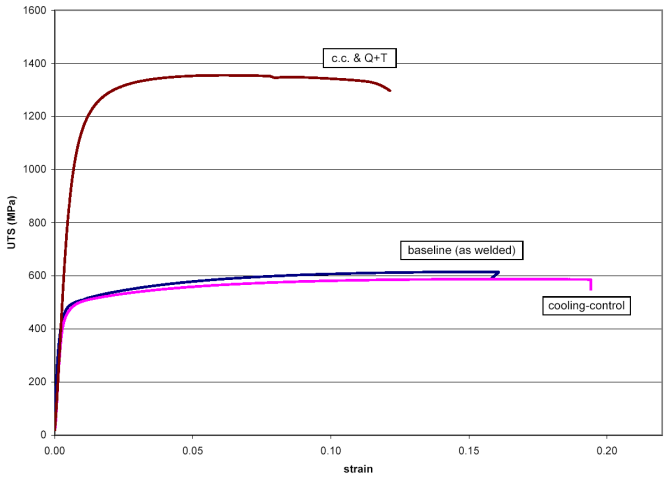

FIG. 17. Typical Stress-Strain plots for Seam-Welded ∅28.6 x 0.5mm UNS41000 Tubing.

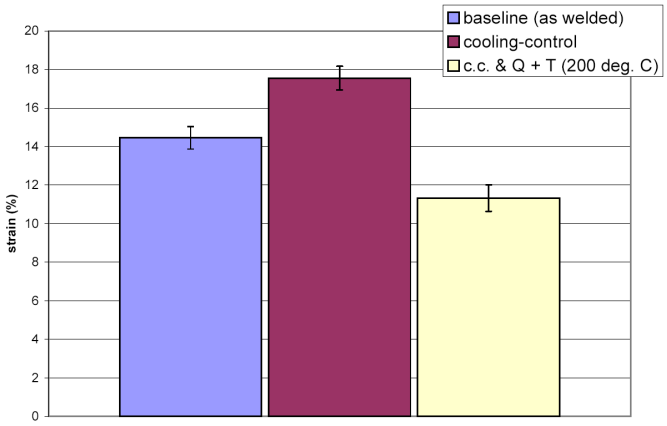

FIG. 18. Comparison of Maximum Strains at fracture for Seam-Welded ∅28.6 x 0.5mm UNS41000 Tubing, average results for 16 trials.

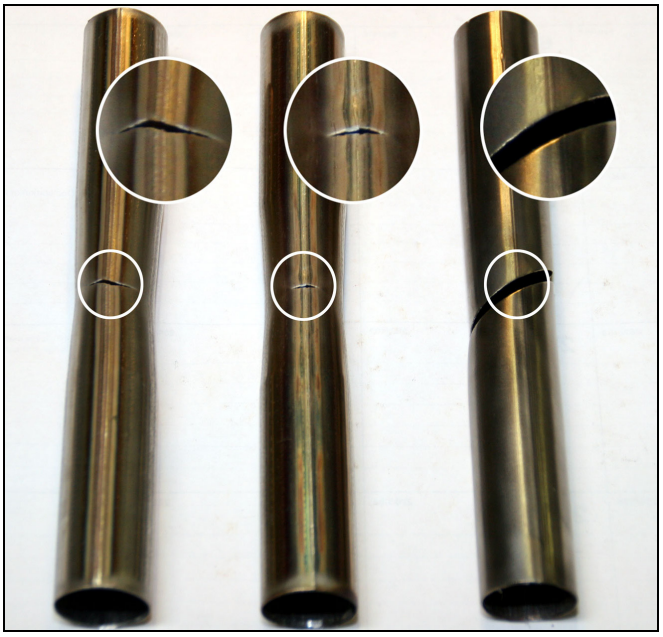

FIG. 19. Typical tensile test tube specimens. From left: as welded; cooling-controlled; C.C. Q+T hardened.

Figure 20 shows typical tube test specimens after flange testing. Clearly visible is the HAZ-base metal interface crack in the as-welded sample, whereas the controlled-cooling specimen is free from splits. The Q+T hardened samples exhibit splitting in the base metal, far away from the HAZ and weld zone.

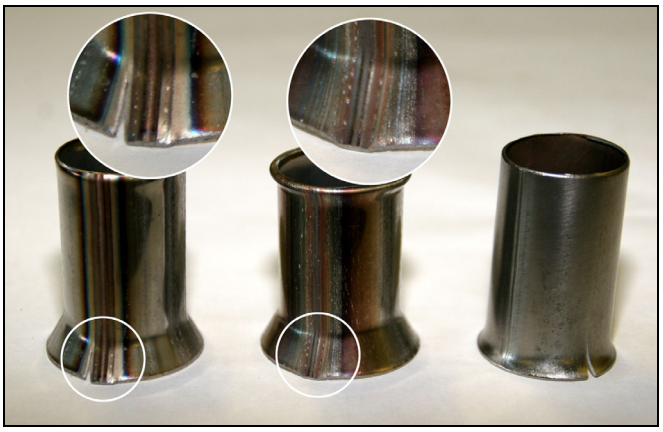

FIG. 20. Typical ASTM A513 ring flare-test tube specimens. From left: as welded; cooling-controlled; C.C. Q+T hardened.

CONCLUSION

A novel method of improving weld ductility based on induction heat treatment of flat butt-joint high-speed autogenous GTAW sheets has been presented. The post-weld ductility of annealed type 410 MSS (UNS 41000), 0.5mm to 2.0mm thick, has shown to be improved by supplemental heating of the HAZ immediately following weld pool solidification. The following conclusions can be drawn from the study:

- Applying optimum cooling-control methods on the weld seam results in an increase in maximum strain at fracture and a corresponding decrease in ultimate tensile strength when compared to as-welded specimens.
- Greatest benefits were observed by reheating the weld seam to the A_{C1} temperature after the weld was allowed to cool below the M_S temperature.
- Improvements in ductility were more marked in thicker gauges.
- Strength levels, after a Q+T air-quench hardening cycle, were not affected by the cooling-control process.
- The as-welded HAZ microhardness is reduced significantly with the addition of the cooling-control process.
- Applying optimal cooling-control parameters to a seam-welded tube mill increases formability of MSS tubing.

ACKNOWLEDGMENTS

The author would like to thank the following individuals:

Mr. Ed McCrink – KVA Incorporated

Mr. Mike Maj – Ford Motor Company

Mr. Shyamal Das – Ford Motor Company

REFERENCES

1. 1. Tsai, C. L., and Tso, C. M. ASM Handbook, Volume 6, 10th edition, Welding, Brazing and Soldering, American Society for Metals, Ohio, 1993
2. Watson, N. M., “Laser welding of structural steel with wire feed,” Research Report, The Welding Institute, England, 1985
3. Bagger, C., Sorensen, J. I., and Olsen, F. O., “Induction heat treatment of laser welds,” Journal of Laser Applications, Volume 15, Number 4, Laser Institute of America, Florida, 2003
4. Semiatin, S. L., and Stutz, D. E., Induction Heat Treatment of Steel, American Society for Metals, Ohio, 1986
5. Lippold, J. C., and Kotecki, D. J., Welding Metallurgy and Weldability of Stainless Steels, John Wiley & Sons, New Jersey, 2005

CONTACT

Daniel Codd - dcodd@kvastainless.com

About KVA

Located in southern California, KVA Incorporated is focused on developing and promoting structural applications for martensitic stainless steels in various industries. KVA’s president, Mr. Ed McCrink, has over 50 years experience working with and processing hardenable alloys. Mr. McCrink founded Hi-Temp, Inc. in 1953 and grew the company to become one of the largest processors of martensitic stainless steels in North America. KVA’s R&D efforts are dedicated to developing, promoting and licensing intellectual property and martensitic stainless processing know-how arrive at cost-effective, superior mechanical and structural solutions.

ABBREVIATIONS

A_{C1}: lower critical temperature; austenite starts to form

A_{C3}: upper critical temperature; fully austenitized

C.C.: cooling-control

AHSS: advanced high strength steels

GTAW: gas tungsten arc welding

HAZ: heat affected zone

M_S: martensite start temperature

MSS: martensitic stainless steels

PWHT: post weld heat treatment

Q+T: quench and temper heat treatment